Contents list available at IJRED website

International Journal of Renewable Energy Development

Journal homepage: https://ijred.undip.ac.id

Research Article

Computational prediction of green fuels from crude palm oil in fluid catalytic cracking riser

Agus Prasetyo Nuryadi[a*], Widodo Wahyu Purwanto[b], Windi Susmayanti[c], Himawan Sutriyanto[a], Bralin Dwiratna[a], Achmad Maswan[a]

[a]*Research Center for Energy Conversion and Conservation, National Research and Innovation Agency, South Tangerang, Indonesia*

[b]*Department of Chemical Engineering, Faculty of Engineering, Universitas Indonesia, Depok, 16424, Indonesia*

[c]*Department of Chemistry, Pharmaceutical Sciences Programs, Faculty of Medicine, Sultan Agung Islamic of University, Semarang, Indonesia*

Abstract. Fluid catalytic cracking could convert crude palm oil into valuable green fuels to substitute fossil fuels. This study aimed to predict the phenomenon and green fuels yield in the industrial fluid catalytic cracking riser using computational fluid dynamics. A three-dimensional transient simulation using the Eulerian-Lagrangian with the multiphase particle-in-cell is to investigate reactive gas-particle hydrodynamics and the four-lump kinetic network model with the rare earth-Y catalyst for crude palm oil cracking behaviors. The study results show that the fluid and catalyst velocity profile increase in the middle of the riser reactor because the cracking reaction process that produces OLP and Gas products has a lighter molecular weight. The endothermic reaction causes the temperature profile to decrease because the heat of the reaction comes from the catalyst. This analysis shows that the simulation accurately predicts green fuel products from crude palm oil. As a result, the crude palm oil conversion, organic liquid product yield, and Gas yield correspond to 70 wt%, 28.8 wt%, and 27.5 wt%, respectively. Compared to the experimental study, the computational prediction of yield products showed good agreement and determined the optimal riser dimension. The methodology and results are guidelines for optimizing the FCC riser process using CPO.

Keywords: CFD, CPO, Gas-particle, Green fuels, Riser, Rare earth-Y catalyst

Received: 3rd May 2023; Revised: 4th August 2023; Accepted: 16th August 2023; Available online: 23rd August 2023

1. Introduction

Fluid catalytic cracking (FCC) has been in commission for almost a century. Numerous advanced technologies have been adopted to meet changing market requirements and address obstacles arising from the need to refine progressively unprocessed petroleum (Sadeghbeigi, 2020). In the past few decades, there has been consistent advancement in FCC technology. This process breaks down the larger hydrocarbon molecules into smaller ones and producing valuable products (Miao *et al.*, 2021; Otten-Weinschenker and Mönnigmann, 2022). The FCC has three main reactors, namely the riser, stripper, and regenerator, with the riser being the primary reactor where the catalytic cracking reaction occurs (Selalame *et al.*, 2023). Liquid feed, preheated beforehand, is inserted through nozzles into the riser reactor to undergo an atomization process, creating fine droplets. These droplets then collide with a hot catalyst and undergo an endothermic reaction and evaporating (Sadeghbeigi, 2020; Du *et al.*, 2022). The cracking process takes place over a length of approximately 3-4 meters and the process involves three phases: the particle/catalyst phase, the liquid/feedstock phase, and the gaseous phase from the reaction products. Once the process is complete, only two phases remain in the middle of the riser: the catalyst phase and a mixture of hydrocarbon vapor and steam (Zhong *et al.*, 2022; Zhang *et al.*, 2023).

The FCC primarily employs VGO or fossil fuels as feedstock. However, there is now an opportunity to utilize CPO for producing green fuels through FCC. Green fuels, also referred to as renewable or alternative fuels, have significantly lower, or even zero, net carbon emissions. They not only offer a means to diversify our energy sources but also help reduce our reliance on finite fossil fuel resources (Cabrera-Jiménez *et al.*, 2022; Grahn *et al.*, 2022; Osman *et al.*, 2022). Furthermore, Indonesia has potential because of produces the enormous amount of CPO in the world (Papilo *et al.*, 2022). The Indonesian government aims to decrease the import of fossil fuels as part of its efforts to reduce the trade deficit. They plan to achieve this by producing green fuels, particularly by increasing the production of palm oil (Sugiyono *et al.*, 2020).

Several studies have described the conversion of biomass into green fuels through catalytic cracking. ZSM-5 and Y-Re-16 catalysts were used on Palm oil to produce organic liquid products (OLP), resulting in 12.1% of gasoline, 8.9% of kerosene, and 71.4% of diesel (Onlamnao, Phromphithak and Tippayawong, 2020). Drop-in green fuel processes using SO_4^{2-}/TiO_2-ZrO_2 catalysts produces >50% green diesel, >32% biogasoline, and <11% heavy fraction, catalysts can be used based on the desired product (Zhang *et al.*, 2020). The cracking

* Corresponding author
Email: agus130@brin.go.id (A.P. Nuryadi)

https://doi.org/10.14710/ijred.2023.54032
ISSN: 2252-4940/© 2023.The Author(s). Published by CBIORE

processing of CPO using Ni and Co impregnation on zeolite HY demonstrates the role of each metal is very significant for further catalyst advancement for the conversion of palm oil to biofuel (Istadi *et al.*, 2021). HCl/γ-Al_2O_3 and HCl/Ni/γ-Al_2O_3 catalysts for cracking palm oil produced biogasoline 6.4%, bioavtur 33.8%, and green diesel 20.3% (Dewanti, Rasyid and Kalla, 2022). The conversion of off grade CPO into biogasoline through catalytic cracking is accomplished using heterogeneous catalysis, and the effectiveness of the α-Fe_2O_3 active site can be enhanced by incorporating cobalt (Co) and molybdenum (Mo) through metal impregnation (Santoso *et al.*, 2023). CPO hydrocracking refer to the two reaction models: the four-lump model and the six-lump model (Hasanudin *et al.*, 2020). The cracking reaction in the riser reactor involves many compounds and reactant products, making it easier to group them into lumps. The three-lump kinetic model (feedstock, gas-oil, and coke) was first developed in FCC kinetic modeling, then the Four-lump model with gas oil is separated into three components, gasoline, gas, and coke. More lumps are added to get higher accuracy in the kinetic model (Chen *et al.*, 2020).

The gas-solid phenomenon in the riser and the cracking reaction phenomenon, a numerical study is needed. It is impossible to do it experimentally due to cost and safety factors. The computational fluid dynamics (CFD) analysis is necessary for FCC development. Detailed experimental investigations have been prevented in the industrial FCC risers due to the presence of disperse catalyst, heat transfer, and reactions of cracking. The gas-particle simulations in CFD are conducted using the E-E (Eulerian-Eulerian) and E-L (Eulerian-Lagrangian) approaches. The E-E, TFM, assumes that a particle can be treated like a liquid, allowing its gas and particle to interpenetrate as continuous phases (Zhong *et al.*, 2020; Yu *et al.*, 2021). However, this approach disregards the particle by describing it as a dispersed phase. Therefore, other methods, such as E-L approaches, DEM (Discrete Element Method) (Gu *et al.*, 2023), Discrete Particle Method (DPM) (Koyunoğlu *et al.*, 2023), and MPPIC (Multiphase Parcel-in-Cell) (Du *et al.*, 2022) can be employed to overcome this limitation.

The complexity of DEM is computational and it is appropriate for small-scale laboratory settings with a limited number of particles (Gu *et al.*, 2023; Horio *et al.*, 2023). On the other hand, DPM utilizes velocity and position monitoring of the particle, similar to DEM, but it does not have the capability to provide detailed information on particle sizes and clusters in the composition. In comparison, the MPPIC method utilizes the Liouville equation to calculate the time evolution of the particle distribution function (Torres Brauer, Serrano Rosales and de Lasa, 2021), enabling the simulation of particle clusters that are suitable for modeling powder hydrodynamics and catalysts. The main purpose of this study was to determine the dynamic behavior of gas and particles, as well as the performance of a commercial scale riser reactor with CPO as feedstock. Computational gas-solid prediction with MPPIC and six upward nozzles was applied. The four-lump kinetic base model with the rare earth-Y (REY) catalyst was adopted to represent the cracking reaction network with CPO as the feedstock.

2. Gas–particle

The pneumatic transport fluidization method is used to find the initial dimensions of a riser reactor is shown in Fig. 2. The simulation was conducted riser reactor to study the interaction between particles catalyst and CPO in industrial FCC riser. The governing equations utilized for this approach allowed for the simulation of both disperse particles and reactions. A thorough explanation and confirmation of the MPPIC model is also provided (Andrews and O'Rourke, 1996):

2.1 Governing Equations

The mass balance equation:

$$\frac{\partial \varepsilon_g \rho_g}{\partial t} + \nabla . \ (\varepsilon_g \rho_g u_g) = 0 \quad (1)$$

The first term is the mass accumulation rate, and the second term is the convection term.

The gas momentum equation:

$$\frac{\partial (\varepsilon_g \rho_g u_g)}{\partial t} + \nabla . \ (\varepsilon_g \rho_g u_g u_g) = -\nabla P + \varepsilon \rho_g g + \nabla . \varepsilon_g \tau_g - F \quad (2)$$

Where the first term is the change in the inertial force of unsteady acceleration, the second term is the difference of inertial force in the convection acceleration. Then the transition of force. The fourth term is the body force, the fifth term is the change of viscous, and the sixth term, F, is the gas and the particles in momentum exchange.

$$F = \iiint f V_p \rho_p \left[\beta \left(u_f - u_p \right) - \frac{\nabla p}{\rho_p} \right] dV_p d\rho_p du_p \quad (3)$$

f is the Liouville equation that describes the change in time to the particle distribution function, β is the EMMS drag model (Dymala, Wytrwat and Heinrich, 2021; Pakseresht *et al.*, 2023), $\boldsymbol{u_f - u_p}$ is the slip velocity. The equation of momentum for the gas and particle is a connector between the equations in the gas and the particle where to predict the movement of particles by the Lioville equation.

The gas species transport equation:

$$\frac{\partial \varepsilon_g \rho_g Y_{g,i}}{\partial t} + \nabla . \ (\varepsilon_g \rho_g u_g Y_{g,i}) = \nabla . \ (\varepsilon_g D \rho_g \nabla Y_{g.i}) + \delta m_{i,chem} \quad (4)$$

$Y_{g,i}$ is the gas species, the first term donates the mass accumulation rate, the second term represent the convection term, for third term is the diffusion term from the Schmidt number correlation with D, Sc = 0.9. $\delta m_{i,chem}$ depicts a chemical source term.

$$S_C = \frac{\mu}{\rho_f D}$$

The energy conservation equation:

$$\frac{\partial (\varepsilon_g \rho_g h_g)}{\partial t} + \nabla . \ (\varepsilon_g \rho_g h_g u_g) = \nabla . (\varepsilon_g q) + \varepsilon_g \left(\frac{\partial p}{\partial t} + u_g . \nabla_p \right) + \dot{q}_D + \dot{Q} + S_h \quad (5)$$

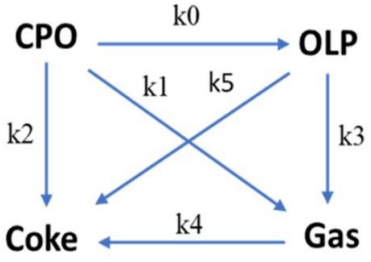

Fig 1. 4-lump FCC kinetic model reaction (Bhatia, Leng and Tamunaidu, 2007)

Table1
Activation energies and frequency factors of CPO with four-lump kinetic model

Reaction	Ea (kJ/kmol)	A
CPO --> OLP	42.659	26.8
CPO --> Coke	30.329	0.01
CPO --> Gas	35.672	3.97
OLP --> coke	21.018	0.5
Gas --> Coke	10.273	0.02

The first term is energy accumulation, and the second term is convection transfer, the third is conduction transfer, the fourth is heat dissipation, and the fifth term is $\dot{Q} + S_h$ additional heat from the hot catalyst, $\dot{q}_D$ is the enthalpy of heat diffusion. $\dot{Q}$ is the endothermic of the cracking reaction ($\dot{Q} = \sum_{j=1}^{n} r_j Q_{rj}. Q_{rj}$) is the heat of reaction from kinetics taken 4-lump. Conservative energy transfer from the particle phase (S_h) to the fluid phase. whereas, r_j describes the reaction rate for component j.

2.2 Kinetic cracking model

The four-lump kinetic model describes the CPO cracking reaction, and the components of the system are CPO, OLP, Gas, and coke are shown in Fig. 1. The rate at which reactant j is consumed per unit of catalyst can be described (Pachovsky and Wojciechowski, 1975).

$$-r = k_j(\frac{C_j}{C_{jo}})^n C_j \varepsilon_s \varphi \qquad (6)$$

C_j is the *j* component concentration, and C_{jo} is the initial purified component j concentration. k_j denotes the pre-exponential factor for a specific temperature. CPO reaction, the value of n is 1, while it is 0 for all other reactions.

$$k_j = k_{jo}\exp(\frac{-E_j}{RT}) \qquad (7)$$

The full expression for the rate of component j can be expressed as follows:

$$-r = k_{jo}\left[\frac{C_j RT}{\varepsilon_g P}\right]^n \exp\left[\frac{-E_j}{RT}\right] C_j \varphi \varepsilon_P \qquad (8)$$

R, T, and P denote the universal gas constant, the temperature of the vapors, and the pressure. The rate expression for equation 8 supposes that the function φ, which accounts for factors like coke coverage, pore occlusion, and the effect of pore occlusion on diffusion, is responsible for catalyst deactivation. Four-lump CPO kinetic model as data input reference on this simulation (Bhatia, Leng and Tamunaidu, 2007). The kinetics model of CPO and the REY catalyst with diameter 150 −200 μm and 5 CTO g.g^{-1} (ratio catalyst to oil) was chosen because it has the most optimal product yield. Table 1 describes the activation energies and frequency factors of CPO with the 4-lump kinetics model as input variables for equations 6-7.

$$Conversion\ (wt\ \%) = \frac{Gas\ (\frac{kg}{s}) + OLP\ (\frac{kg}{s})}{CPO\ (\frac{kg}{s})} \times 100\% \qquad (9)$$

$$Yield\ Product\ (wt\ \%) = \frac{Product\ (\frac{kg}{s})}{CPO\ (\frac{kg}{s})} \times 100\% \qquad (10)$$

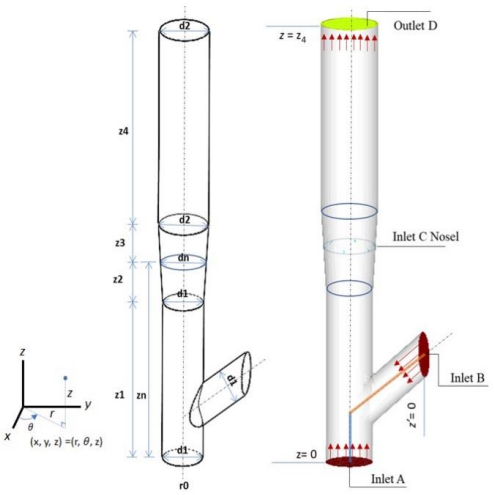

Fig 2. Initial dimensions of riser.

Performance of reactor is defined as conversion and product yield by Equations 9 and 10 (Bhatia, Leng and Tamunaidu, 2007).

3. Numerical setup

The geometry with boundary and initial conditions shown in Fig. 2 has a capacity of 4000 tons/day. Inlet A and Inlet B are designated as "velocity inlets" for boundary conditions, while the riser outlets are designated as "outlets" for Outlet D, where the steam inlet and catalyst inlet are located on the inclined pipe. The gas phase is subject to a no-slip condition at the wall boundary. The CPO feed inlet is designated as "inject" for Inlet C, with the six upward nozzles and angles is 30°. For detail dimension and parameter are shown in Table. 1.

Equations 1-5 were used to describe the fluid field, and a numerical solution was obtained using the finite volume method. The velocity and pressure were adjusted using a SIMPLE. To achieve numerical convergence was selected for each time step, while using a small time interval of 0.0001 seconds. The simulation was conducted transient with 120 seconds and the riser used a structured grid type with a hexahedral mesh. The independence and refinement tests have been used to check the mesh and the independence test involved comparing the results of three different mesh configurations, Mesh 1: 354,000 (number of meshes), 0.077 (grid distance), Mesh 2: 295,000 (number of meshes), 0.082 (grid distance), and Mesh 3: 236,000 (number of meshes), 0.089 (grid distance). Using an independent test equation, the comparison of these meshes shows that the grid-convergence index (GCI) is 0.61 (with an allowed value of 0.5 < 1), indicating that the three meshes are independent and do not require a refinement test (Boache, 1994; Roache, 1997).

4. Simulation results and discussion

The results of simulation depict the cracking reaction, including the momentum equation which reflects the velocity and void fraction. The energy equation shows the temperature, while the mass equation shows the product of the cracking reaction (Selalame *et al.*, 2022). The displayed simulation results are from transient simulations spanning 0 to 21 seconds, while the analysis is presented for time intervals of 9, 12, and 15 seconds due to their significant differences.

Table 2
Initial and boundary conditions

Parameter		value
Pre-lift zone diameter,	d1 (m)	0.59
Pre-lift zone height,	z1 (m)	2.3
	z2 (m)	1.5
	z3 (m)	1.5
Nozzle height	zn (m)	5.3
Diameter of riser,	d2 (m)	0.8
Height of riser,	z4 (m)	52.35

Parameter	value
Initial condition	
Steam temperature, (T) K	593.13
Pressure steam, (P) Pa	166713
Inlet A (steam)	
Flow rate, kg/s	0.8
Pressure, (P) Pa	166713
Temperature, (T) K	593.13
Inlet B	
Flow rate catalyst, kg/s	210
catalyst temperature, (T) K	973
Flow rate steam, kg/s	0.4
Steam Temperature, (T) K	593.13
Inlet C (Injection)	
Flow rate CPO, kg/s	42
Number of nozzles	6
Nozzle angle	30^{O} upward

First, CPO is introduced into the gas-solid mixture through six nozzles positioned at a 30 degrees upward angle from the bottom of the riser reactor. This injection reduces the empty space within the mixture, leading to an upsurge in the velocity of both the gas phase and catalyst particles within the central atomization area of the riser. The introduction of hydrocarbon vapor further contributes to this process by increasing the velocity of the gas-solid mixture. As the droplets vaporize, they initiate cracking reactions, leading to an increase in the gas phase volume and the production of lighter gases. These combined effects result in heightened gas velocities in the upper and middle sections of the riser reactor, as depicted in Fig 3. The gas phase velocity illustrates that once the CPO spray completely vaporizes into the gas mixture, the flow pattern of the gas phase closely resembles plug flow. To prevent undesired

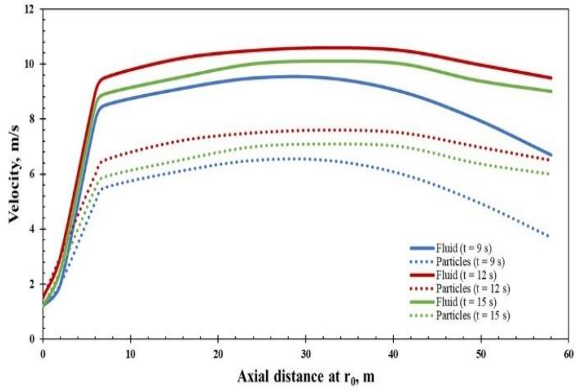

Fig 3. Velocity graph of the fluid and catalyst in the axial direction at r_0

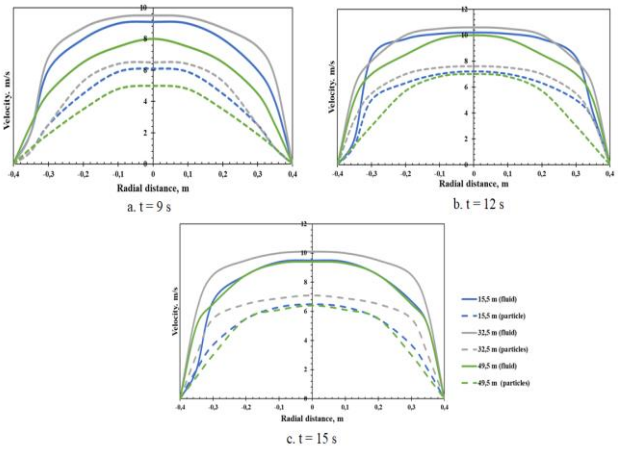

Fig 4. Velocity in the fluid and catalyst in the radial direction

cracking reactions associated with back mixing, the implementation of six atomizers has proven effective in promoting plug flow and minimizing these reactions.

The change in velocity resulting from the cracking reaction occurs when the CPO feed is depleted, leading to the formation of products, namely Gas and OLP. These products have lower density, causing an increase in velocity. At a distance of 32.5 meters, there is a velocity decrease due to the effects of gravity and a reduction in the rates of cracking reactions, which is caused by catalyst deactivation. Catalysts become less effective over time as they accumulate coke during the cracking process. While the presence of coke contributes to catalyst deactivation, assessing catalyst activity based on coke usage was found to be challenging. At a distance of 15.5 meters, the radial graph exhibits asymmetry due to the catalyst inlet being on the left side, resulting in catalyst clustering along the left wall, as shown in Fig. 4.

The supercritical steam and hot catalyst entering the riser form a mixture with CPO as hydrocarbons. The high temperature and pressure in the riser cause the heavy hydrocarbons to vaporize rapidly, forming gas phase products. These products contribute to an increase in fluid velocity (Chen *et al.*, 2021; Yu *et al.*, 2021; Du *et al.*, 2022; Selalame *et al.*, 2023). The steam from the bottom and the injection feed of the riser is at high pressure. As it travels upward, there is a pressure drop along the length of the riser (Chang *et al.*, 2020). As the pressure decreases, the velocity increases to maintain energy conservation (Selalame *et al.*, 2023). Increasing velocity affected to volume fraction is shown in Fig. 5. The effect of increasing velocity on the volume fraction is shown in Fig. 5. The volume fraction changes over the simulation time due to the increased

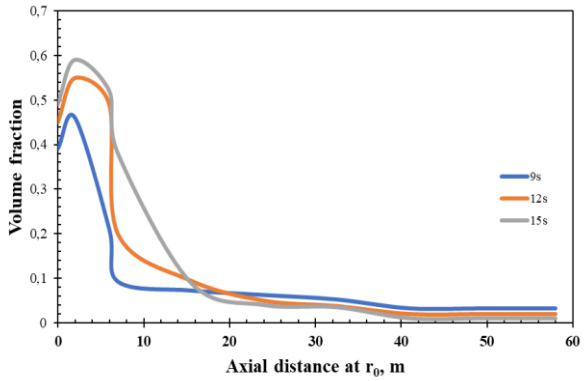

Fig 5. volume fraction in the axial direction at r_0

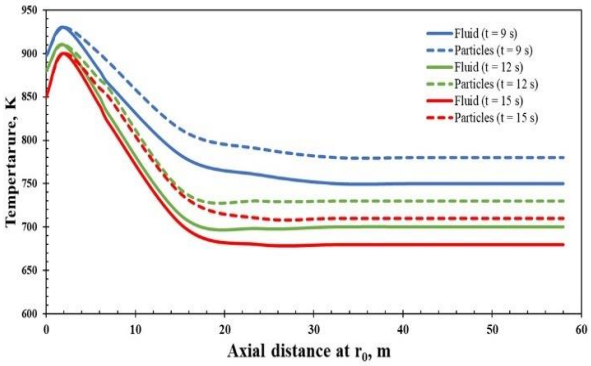

Fig 6. The temperature contours and graph of the fluid and catalyst in the axial direction at r_0

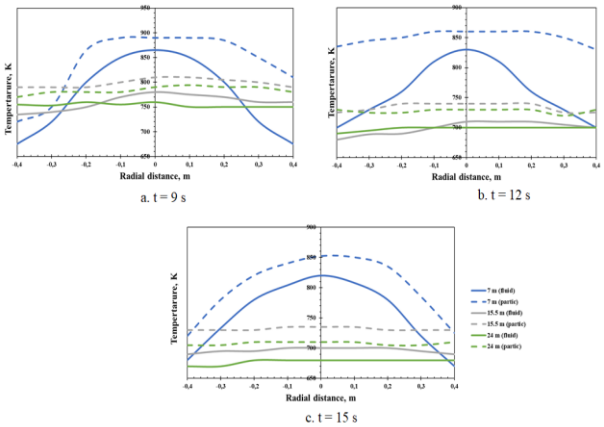

Fig 7. The temperature of the fluid and the catalyst is in the radial direction

velocity resulting from the cracking reaction (Akhavan and Blaser, 2021).

The angle at which the feed is injected is crucial for the gas and solids flow, as well as the reaction efficiency within the riser reactor. In addition to the injection angle, the velocity at which the feed is injected also impacts the overall reactor performance. Six nozzles with an upward angle of 30 degrees were selected, as previous studies have shown that this configuration can result in increased product yield and enhanced catalyst hydrodynamics stability in the reactor riser. The presence of a fully developed radial velocity profile within the reactor riser validates the appropriateness of this chosen configuration, as illustrated in Fig. 4. Furthermore, the uniform temperature distribution depicted in the radial temperature profile demonstrates the positive impact on the cracking reaction process is shown in Fig. 7.

The temperature drops due to the interaction between the hot catalyst and CPO, and supercritical steam is depicted in Fig. 6. The cracking reaction in the riser reactor is endothermic, with the only heat source being the heat of the catalyst. The temperatures decrease at 9 seconds, 12 seconds, and 15 seconds, and then remain stable at a height of 35 m, with an average temperature difference of around 30 K between the catalyst and the fluid. Additionally, the graph shows that the temperature begins to stabilize after a height of 24 m and remains constant at 34 m. Temperature variations in the simulations at the heights of 7 m, 15.5 m, and 24 m for the simulation results at 9 seconds, 12 seconds, and 15 seconds on the radial axis are presented in Fig. 7. From the radial graph, there is still a temperature fluctuation at height of 7 m with the highest temperature at the center of the reactor and the lowest at the reactor wall. However, temperatures at 15.5 m and 24 m are relatively uniform.

Temperature reduction in the riser reactor is generally attributed to several factors. Firstly, the cracking of heavy hydrocarbon molecules into lighter ones is highly endothermic, necessitating heat for the reaction to proceed. As the feedstock and catalyst enter the riser reactor, heat is absorbed by the cracking reactions, leading to a decrease in temperature (Chen *et al.*, 2021). In the FCC process, the feedstock is mixed with numerous fluidized catalyst particles, which serve as a diluent, lowering the feedstock concentration and overall temperature in the riser reactor. The riser reactor, being a relatively long and narrow vessel where the feedstock and catalyst are mixed and transported, experiences heat loss along its length due to convection, radiation, and contact with the cooler reactor walls, all contributing to the temperature decrease (Akermann, Renze and Schröder, 2022).

The conversion and yield of OLP and Gas products in the axial direction from equations 9 and 10 are shown in Fig. 8a. The OLP yield continued to increase until the 15-second simulation and remained constant. However, it differed for the Gas yield, which peaked at the 12 seconds, then slightly decreased at the 15 second and remained constant. The simulation at 15 seconds exhibited the best conversion and yield of the product. Gas yield is the largest product, as shown in Fig. 8b.

The analysis from the previous study shows that the ratio of the dimensions of the riser is 0.02, this ratio is calculated from the relationship between the height and diameter (Theologos and Markatos, 1993; Ali, Rohani and Corriou, 1997; Derouin *et al.*, 1997; Behjat, Shahhosseini and Marvast, 2011; Zhu *et al.*, 2011), are shown in Table 3. Using ratio and simulation to find the optimal dimensions for a riser reactor, as a result, the height is 37 m and a diameter is 0.8 m with 28.8 wt% yield of OLP and 27.5 wt% yield of Gas. Due accuracy of the simulation analysis results was compared to that of the experimental study results. The simulation is based on the yield of the optimal dimensions, while the experimental study is taken from Bhatia, Leng, and Tamunaidu (2007), as shown in Table 4. The comparison between experimental study and simulation using $(Y_{exp} - Y_{sim})/Y_{exp}$. The tolerance between the experimental and simulation studies has a slight difference. As a result, the comparison demonstrates good agreement.

5. Conclusion

In this work, the CFD approach based on the MPPIC method was applied to study the hydrodynamics, catalytic cracking

Table 3
The ratio of the dimensions of the industrial-scale riser (Theologos and Markatos, 1993; Ali *et al*, 1997; Derouin *et al.*, 1997; Behjat *et al*, 2011; Zhu *et al.*, 2011)

Parameter	Theologos and Markatos, (1993)	Derouin *et al,* (1997)	Ali *et al,* (1997)	Behjat *et al* (2011)	Zhu *et al* (2011)	Zhu *et al* (2011)
Diameter (m)	1.24	1	0.8	0.14	0.8	1
Height (m)	50	35	33	11	33	35
Ratio	0.025	0.029	0.024	0.0127	0.024	0.03

Table 4
The comparison results

Yield product	Simulation (wt%)	Bhatia (%)	Tolerance
OLP	28.8	30.2	0.046
Gas	27.5	36	0.236

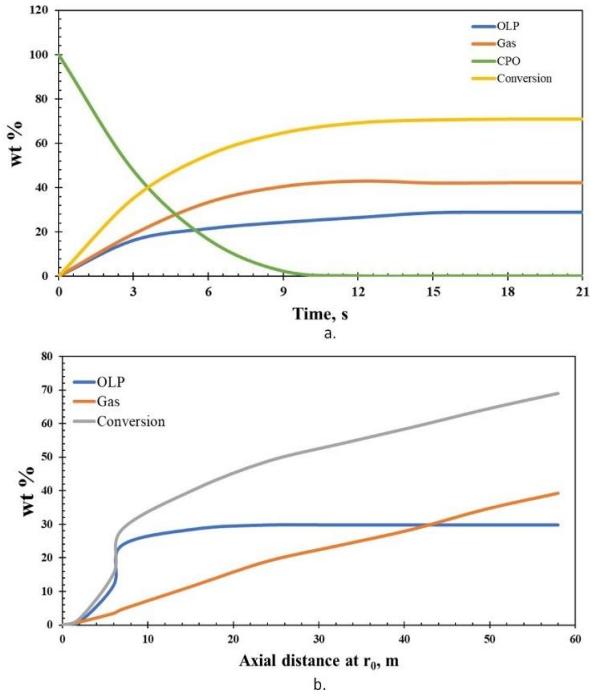

Fig 8. a. The axial conversion and yield by time at r_0, b. The axial conversion and yield at r_0,

reactions characteristics, and heat transfer in FCC riser reactor. The MPPIC had the ability to monitor both gas and catalyst particle stages, and it employed a four-lump kinetic reaction model using a REY catalyst to explain the cracking reactions involving CPO. The accuracy of the computational prediction has been confirmed by comparing it with experimental data, demonstrating its capability to accurately represent the key characteristics of FCC riser behavior. The simulation result that CPO is possible as feedstock in FCC for industrial scale. Simulation of riser reactor using six upward injections shows conversion and yield product distribution were qualified and discussed. Hence, the model has the potential to serve as a tool that aids in the creation, functioning, and management of industrial FCC risers for the purpose of generating green fuels. As future investigation, more lumps of CPO kinetics model and comparison various catalyst should be considered.

Abbreviations

CFD : Computational fluid dynamics
CPO : Crude palm oil
DEM : Discrete Element Method
DPM : Discrete Particle Method
E-E : Eulerian – Eulerian
E-L : Eulerian – Lagrangian
EMMS : The energy minimization multi-scale
FCC : Fluid catalytic cracking
MPPIC : Multiphase particle-in-cell
REY : Rare earth-Y catalyst
TFM : Two fluid model

Acknowledgments

The author would like to thank the National Research and Innovation Agency (BRIN) for facilitating the research.

Author Contributions: A.P.N: Conception, methodology, investigation, writing, resources, validation. W.W.P.; Conception, methodology, guidance, W.S & H.S.; writing editing, administration, B.D; review and validation, A.M; project administration.

Conflicts of Interest: The authors declare no conflict of interest.

References

Akermann, K., Renze, P., & Schröder, W. (2022). Large-eddy simulation for solid particle transport and deposition in a helically rib-roughened pipe using an Euler-Lagrange approach. *Chemical Engineering Science*, *253*, 117557. https://doi.org/10.1016/j.ces.2022.117557

Akhavan, A., & Blaser, P. (2021). CFD Modeling and Liquid Vaporization: Industrial FCC Riser Feed Injection Application. *AIChE Annual Meeting, Conference Proceedings*, *2021-Novem*, 2023.

Ali, H., Rohani, S., & Corriou, J. P. (1997). Modelling and control of a riser type fluid catalytic cracking (FCC) unit. *Chemical Engineering Research and Design*, *75*(4), 401–412. https://doi.org/10.1205/026387697523868

Andrews, M. J., & O'Rourke, P. J. (1996). The multiphase particle-in-cell (MP-PIC) method for dense particulate flows. *International Journal of Multiphase Flow*, *22*(2), 379–402. https://doi.org/10.1016/0301-9322(95)00072-0

Behjat, Y., Shahhosseini, S., & Marvast, M. A. (2011). CFD analysis of hydrodynamic, heat transfer and reaction of three phase riser reactor. *Chemical Engineering Research and Design*, *89*(7), 978–989. https://doi.org/10.1016/j.cherd.2010.10.018

Bhatia, S., Leng, C. T., & Tamunaidu, P. (2007). Modeling and simulation of transport riser reactor for catalytic cracking of palm oil for the production of biofuels. *Energy and Fuels*, *21*(6), 3076–3083. https://doi.org/10.1021/ef070186o

Boache, P. J. (1994). Perspective: A method for uniform reporting of grid refinement studies. *Journal of Fluids Engineering, Transactions of the ASME*, *116*(3), 405–413. https://doi.org/10.1115/1.2910291

Cabrera-Jiménez, R., Mateo-Sanz, J. M., Gavaldà, J., Jiménez, L., & Pozo, C. (2022). Comparing biofuels through the lens of sustainability: A data envelopment analysis approach. *Applied Energy*, *307*, 118201. https://doi.org/10.1016/j.apenergy.2021.118201

Chang, J., Wang, X., Liu, W., Wang, L., & Meng, F. (2020). CFD modeling of hydrodynamics and kinetic reactions in a heavy oil riser reactor: Influence of downward feed injection scheme. *Powder Technology*, *361*, 136–144. https://doi.org/10.1016/j.powtec.2019.10.010

Chen, S., Fan, Y., Kang, H., Lu, B., Tian, Y., Xie, G., Wang, W., & Lu, C. (2021). Gas-solid-liquid reactive CFD simulation of an industrial RFCC riser with investigation of feed injection. *Chemical Engineering Science*, *242*, 116740. https://doi.org/10.1016/j.ces.2021.116740

Chen, Y., Wang, W., Wang, Z., Hou, K., Ouyang, F., & Li, D. (2020). A 12-lump kinetic model for heavy oil fluid catalytic cracking for cleaning gasoline and enhancing light olefins yield. *Petroleum Science and Technology*, *38*(19), 912–921. https://doi.org/10.1080/10916466.2020.1796701

Derouin, C., Nevicato, D., Forissier, M., Wild, G., & Bernard, J.-R. (1997). Hydrodynamics of Riser Units and Their Impact on FCC Operation. *Industrial & Engineering Chemistry Research*, *36*(11), 4504–4515. https://doi.org/10.1021/ie970432r

Dewanti, A. T., Rasyid, R., & Kalla, R. (2022). Effect of HCl/γ-Al2O3 and HCl/Ni/γ-Al2O3 Catalyst on The Cracking of Palm Oil. *Jurnal Kimia Valensi*, *8*(2), 190–198. https://doi.org/10.15408/jkv.v8i2.25774

Du, Y., Chen, X., Li, S., Berrouk, A. S., Ren, W., & Yang, C. (2022). Revisiting a large-scale FCC riser reactor with a particle-scale model. *Chemical Engineering Science*, *249*, 117300. https://doi.org/10.1016/j.ces.2021.117300

Dymala, T., Wytrwat, T., & Heinrich, S. (2021). MP-PIC simulation of circulating fluidized beds using an EMMS based drag model for Geldart B particles. *Particuology*, *59*, 76–90. https://doi.org/10.1016/j.partic.2021.07.002

Grahn, M., Malmgren, E., Korberg, A. D., Taljegard, M., Anderson, J. E., Brynolf, S., Hansson, J., Skov, I. R., & Wallington, T. J. (2022). Review of electrofuel feasibility - Cost and environmental impact. *Progress in Energy*, *4*(3). https://doi.org/10.1088/2516-1083/ac7937

Gu, C., Zhao, H., Xu, B., Yang, J., Zhang, J., Du, M., Liu, Y., Tikhankin, D., & Yuan, Z. (2023). CFD-DEM simulation of distribution and agglomeration characteristics of bendable chain-like biomass particles in a fluidized bed reactor. *Fuel*, *340*, 127570. https://doi.org/10.1016/j.fuel.2023.127570

Hasanudin, H., Rachmat, A., Said, M., & Wijaya, K. (2020). Kinetic model of crude palm oil hydrocracking over ni/mo zro2 –pillared bentonite catalyst. *Periodica Polytechnica Chemical Engineering*, *64*(2), 238–247. https://doi.org/10.3311/PPch.14765

Horio, M., Kai, T., Tsuji, T., & Hatano, H. (2023). Fluidization centennial and the decades of research and development in Japan. *Powder Technology*, *415*, 118093. https://doi.org/10.1016/j.powtec.2022.118093

Istadi, I., Riyanto, T., Buchori, L., Anggoro, D. D., Pakpahan, A. W. S., & Pakpahan, A. J. (2021). Biofuels production from catalytic cracking of palm oil using modified hy zeolite catalysts over a continuous fixed bed catalytic reactor. *International Journal of Renewable Energy Development*, *10*(1), 149–156. https://doi.org/10.14710/ijred.2021.33281

Koyunoğlu, C., Gündüz, F., Karaca, H., Çınar, T., & Soyhan, G. G. (2023). Developing an adaptive catalyst for an FCC reactor using a CFD RSM, CFD DPM, and CFD DDPM–EM approach. *Fuel*, *334*, 126550. https://doi.org/10.1016/j.fuel.2022.126550

Miao, P., Zhu, X., Guo, Y., Miao, J., Yu, M., & Li, C. (2021). Combined mild hydrocracking and fluid catalytic cracking process for efficient conversion of light cycle oil into high-quality gasoline. *Fuel*, *292*, 120364. https://doi.org/10.1016/j.fuel.2021.120364

Onlamnao, K., Phromphithak, S., & Tippayawong, N. (2020). Generating organic liquid products from catalytic cracking of used cooking oil over mechanically mixed catalysts. *International Journal of Renewable Energy Development*, *9*(2), 159–166. https://doi.org/10.14710/ijred.9.2.159-166

Osman, A. I., Mehta, N., Elgarahy, A. M., Hefny, M., Al-Hinai, A., Al-Muhtaseb, A. H., & Rooney, D. W. (2022). Hydrogen production, storage, utilisation and environmental impacts: a review. *Environmental Chemistry Letters*, *20*(1), 153–188. https://doi.org/10.1007/s10311-021-01322-8

Otten-Weinschenker, J., & Mönnigmann, M. (2022). Robust optimization of stiff delayed systems: application to a fluid catalytic cracking unit. *Optimization and Engineering*, *23*(4), 2025–2050. https://doi.org/10.1007/s11081-021-09654-8

Pachovsky, R. A., & Wojciechowski, B. W. (1975). Temperature effects on conversion in the catalytic cracking of a dewaxed neutral distillate. *Journal of Catalysis*, *37*(1), 120–126. https://doi.org/10.1016/0021-9517(75)90140-2

Pakseresht, P., Yao, Y., Fan, Y., Theuerkauf, J., & Capecelatro, J. (2023). A critical assessment of the Energy Minimization Multi-Scale (EMMS) model. *Powder Technology*, *425*, 118569. https://doi.org/10.1016/j.powtec.2023.118569

Papilo, P., Marimin, M., Hambali, E., Machfud, M., Yani, M., Asrol, M., Evanila, E., Prasetya, H., & Mahmud, J. (2022). Palm oil-based bioenergy sustainability and policy in Indonesia and Malaysia: A systematic review and future agendas. *Heliyon*, *8*(10), e10919. https://doi.org/10.1016/j.heliyon.2022.e10919

Roache, P. J. (1997). Quantification of uncertainty in computational fluid dynamics. *Annual Review of Fluid Mechanics*, *29*, 123–160. https://doi.org/10.1146/annurev.fluid.29.1.123

Sadeghbeigi, R. (Ed.). (2020). Fluid Catalytic Cracking Handbook (Fourth Edition). In *Fluid Catalytic Cracking Handbook (Fourth Edition)* (Fourth Edi, pp. 1–22). Butterworth-Heinemann. https://doi.org/10.1016/B978-0-12-812663-9.00001-1

Santoso, A., Mulyaningsih, A., Sumari, S., Retnosari, R., Aliyatulmuna, A., Pramesti, I. N., & Asrori, M. R. (2023). Catalytic cracking of off grade crude palm oil to biogasoline using Co-Mo/α-Fe2O3 catalyst. *Energy Sources, Part A: Recovery, Utilization, and Environmental Effects*, *45*(1), 1886–1899. https://doi.org/10.1080/15567036.2023.2183998

Selalame, T. W., Patel, R., Mujtaba, I. M., & John, Y. M. (2022). A Review of Modelling of the FCC Unit. Part I: The Riser. *Energies*, *15*(1). https://doi.org/10.3390/en15010308

Selalame, T. W., Patel, R., Mujtaba, I. M., & John, Y. M. (2023). Effect of vaporisation models on the FCC riser modelling. In A. C. Kokossis, M. C. Georgiadis, & E. Pistikopoulos (Eds.), *33rd European Symposium on Computer Aided Process Engineering* (Vol. 52, pp. 783–788). Elsevier. https://doi.org/10.1016/B978-0-443-15274-0.50125-6

Sugiyono, A., Fitriana, I., Budiman, A. H., & Nurrohim, A. (2020). Prospects for the Development of Green Gasoline and Green Diesel from Crude Palm Oil in Indonesia. *Industrial Science and Technology*, *981*, 202–208. https://doi.org/10.4028/www.scientific.net/MSF.981.202

Theologos, K. N., & Markatos, N. C. (1993). Advanced modeling of fluid catalytic cracking riser-type reactors. *AIChE Journal*, *39*(6), 1007–1017. https://doi.org/10.1002/aic.690390610

Torres Brauer, N., Serrano Rosales, B., & de Lasa, H. (2021). Single bubble in a 3D sand fluidized bed gasifier environment: A CFD-MPPIC simulation. *Chemical Engineering Science*, *231*, 116291. https://doi.org/10.1016/j.ces.2020.116291

Yu, J., Gao, X., Lu, L., Xu, Y., Li, C., Li, T., & Rogers, W. A. (2021). Validation of a filtered drag model for solid residence time distribution (RTD) prediction in a pilot-scale FCC riser. *Powder Technology*, *378*, 339–347. https://doi.org/10.1016/j.powtec.2020.10.007

Zhang, J., Wu, Z., Li, X., Zhang, Y., Bao, Z., Bai, L., & Wang, F. (2020). Catalytic Cracking of Inedible Oils for the Production of Drop-In Biofuels over a SO42−/TiO2-ZrO2 Catalyst. *Energy & Fuels*, *34*(11), 14204–14214. https://doi.org/10.1021/acs.energyfuels.0c02204

Zhang, M., Yang, Z., Zhao, Y., Lv, M., Lan, X., Shi, X., Gao, J., Li, C., Yuan, Z., & Lin, Y. (2023). A hybrid safety monitoring framework for industrial FCC disengager coking rate based on FPM, CFD, and ML. *Process Safety and Environmental Protection*, *175*, 17–33. https://doi.org/10.1016/j.psep.2023.05.004

Zhong, H., Chen, J., Gao, F., Zhang, J., Zhu, Y., & Niu, B. (2022). 3D virtual full-loop CFD simulation of industrial two-stage FCC reaction-regeneration system. *International Journal of Chemical Reactor Engineering*, *20*(11), 1179–1191. https://doi:10.1515/ijcre-2021-0249

Zhong, H., Zhang, J., Liang, S., & Zhu, Y. (2020). Two-fluid model with variable particle–particle restitution coefficient: application to the simulation of FCC riser reactor. *Particulate Science and Technology*, *38*(5), 549–558. https://doi.org/10.1080/02726351.2018.1564094

Zhu, C., Jun, Y., Patel, R., & Wang, D. (2011). Interactions of Flow and Reaction in Fluid Catalytic Cracking Risers. *AIChE Journal*, *59*(4), 215–228. https://doi.org/10.1002/aic.12509